On fracture mechanism of granite saturated with water

E.E. Damaskinskaya, A.G. Kadomtsev, V.S. Kuksenko
Ioffe Physical Technical Institute, Russian Academy of Sciences, St. Petersburg, Russia

1. Introduction

It is known that penetration of a liquid into a rock that gives rise to a pore pressure can play a key role in fracture of rocks [1, 2]. To explain this phenomenon, a dilatancy-diffusion (DD) model [1] based on laboratory experiments on deformation of rocks under high pressures was suggested in the 1970ies. Dilatancy is an increase in volume of a granular substance under deformation. The essence of the model is as follows. The microcracks formed in a rock under high pressures give rise to changes in the physical parameters of the rock, such as the P wave velocity [1, 3], volume, electrical resistance, etc. As water penetrates into cracks, the rock increases in volume and, as a result, the region saturated with water becomes larger, and the pore pressure in cracks arises. This can lead to a sample rupture (and to an earthquake at the large-scale level).

Of great importance for understanding of the process of fracture of rocks is the investigation of spatial distribution of the defects formed under the conditions of penetration of a fluid into this material. There has been few research efforts directed to the solution of this problem. The goal of this paper is to inquire into the mechanism of crack accumulation in water-saturated granite samples and to reveal its difference from crack accumulation in dry granite samples.

2. Experimental

A cylindrical Westerly granite sample (h=109.5 mm, d=76.2 mm) was subjected to loading in the installation described in [4]. Dry samples were deformed under the condition of constant confining pressure (Pc=50 ± 0.2 MPa) and uniaxial loading (Pax). The water-saturated samples were deformed under the conditions of a confining pressure of 50 MPa and pore pressure of 1 MPa. The samples were fully saturated with water prior to deformation. The axial deformation was varied in discrete steps. In the experiments, the axial load and transverse and longitudinal deformations were measured [3].

Crack formation was monitored by detecting acoustic emission signals (AE). As shown earlier, a crack formed in a rock gives rise to the AE signal [5] the

amplitude of which correlates with the crack size [6] and the coordinates of the AE source hypocenter gives information on the crack coordinates. Thus analysis of acoustic emission is a valuable tool for investigation of the fracture development. To detect the AE signals generated during loading, a system consisting of 6 piezoelectric transducer was fixed at the sample (resonance frequency 0.6 MHz). The transducer curvature corresponded to the sample surface shape. The transducer diameter was 6.4 mm. The accuracy of determining the coordinates of the hypocenters of AE sources was 3 mm over the entire sample volume for more than 10^5 signals. The acoustic emission data bases obtained in the experiments were parameters of chronologically successive AE signals. Each signal was characterized by the time of emission, three coordinates of the hypocenter, and amplitude A recalculated to the reference sphere of radius R_f=10 mm.

To analyze the acoustic emission, a statistical criterion of the fracture nucleation site formation was used. This criterion was suggested earlier [7] and used to reveal local fracture nucleation sites at different scales [8]. It was found that simultaneous decrease in the mean time Δt (and spatial Δr) intervals between chronologically successive defects and increase in relevant variation coefficients ($V_{\Delta t}$, $V_{\Delta r}$) points to formation of a fracture nucleation site.

2. Results and discussion

2.1. Fracture development in the dry samples

Fig.1 shows dependences of statistical parameters on time. It can be seen that Δt and $V_{\Delta t}$ vary only slightly during the time period from 0 (start of the experiment) till T1, i.e., the process is quasistationary. A disperse defect accumulation characterized by Δr determined by sample sizes and stable and low $V_{\Delta r}$ occurs. This is illustrated by the distribution of the AE source hypocenters presented in Fig.2a. The fracture nucleation macrosite formation starts from moment T1. This is evidenced by decreases in Δt and Δr and simultaneous increases in $V_{\Delta t}$ and $V_{\Delta r}$ (Fig.1). The localization zone becomes pronounced (Fig.2b). This zone is located in the central part of the sample, nearer to the lateral surface, and has coordinates X=10÷27 mm, Y=4÷20 mm, and Z=89÷120 mm. At T2 an increase in the mean spatial intervals is observed. Defect formation occurs outside the fracture nucleation site, i.e., propagation of a macrocrack begins (Fig.2c).

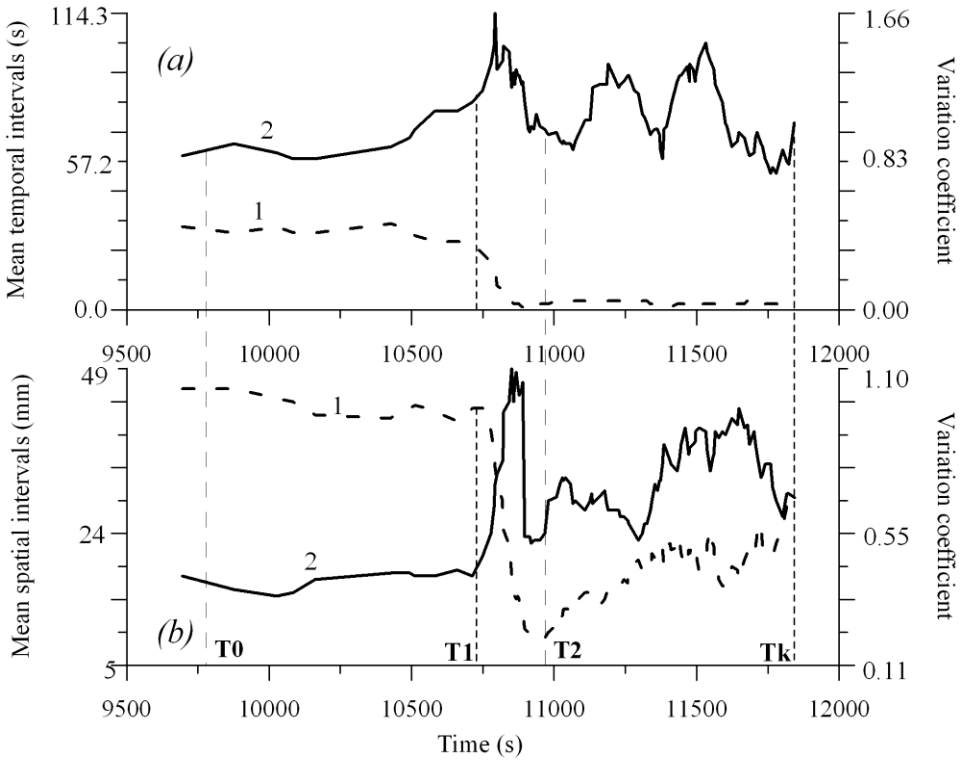

Fig.1. Variations in statistical parameters during deformation of the dry sample:
(a) mean time intervals (curve 1), variation coefficient of time intervals (2);
(b) mean spatial intervals (curve 1), variation coefficient of spatial intervals (curve 2) . (Tk is the moment of time when the experiment was stopped).

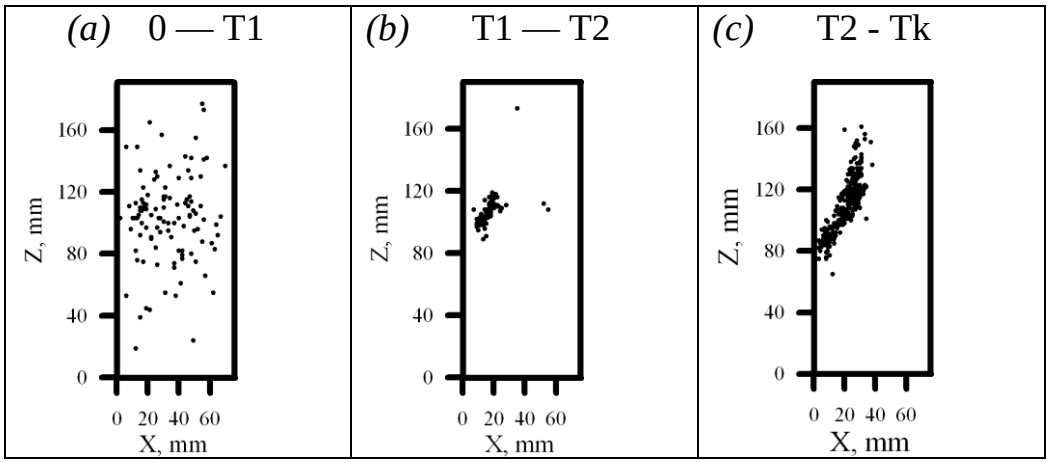

Fig.2. Spatial distribution of coordinates of AE source hypocentres (dry material):
(a) signals detected during time interval 0 - T1 (disperse fracture);
(b) signals detected during time interval T1-T2 (fracture localization);
(c) signals detected during time interval T2-Tk (macrocrack propagation).

2.2. Fracture development in the water-saturated sample

Fig.3 shows variations in the axial load and AE activity. It can be seen that the bursts of AE activity correspond to the moments of stepwise load increases. Of particular interest is the pattern of defect accumulation during the periods of time when deformation and load are nearly unchanged. Three periods were chosen for analysis, i.e., the periods when the load was 76%, 86%, and 95% of the breakdown load (periods I, II, and III, respectively). For each period, graphs of variations in the statistical parameters and spatial distribution of AE signal hypocenters were plotted.

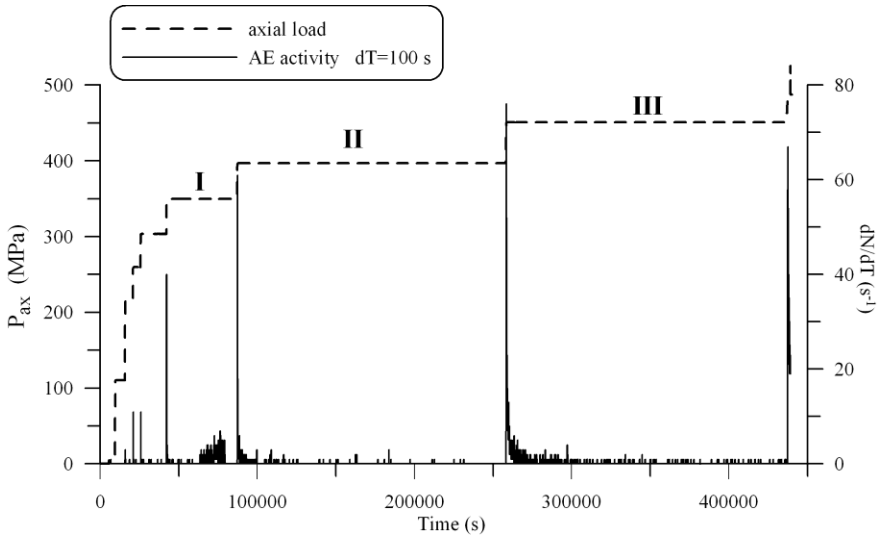

Fig.3. Variations in axial load and AE activity during deformation of the water-saturated sample.

During period I, the mean time interval and variation coefficient vary only slightly till moment T1. After T1, a simultaneous decrease in the time interval and increase in $V_{\Delta t}$ begin. Defect formation occurs in a localized spatial region in the middle part of the sample (Fig.4). As shown in [3], «pressing out» of water from the sample resulting from load increase occurs during this period. This means that the material in the central part of the sample becomes dry, and the pattern of fracture development corresponds to the behavior of fracture of a dry sample.

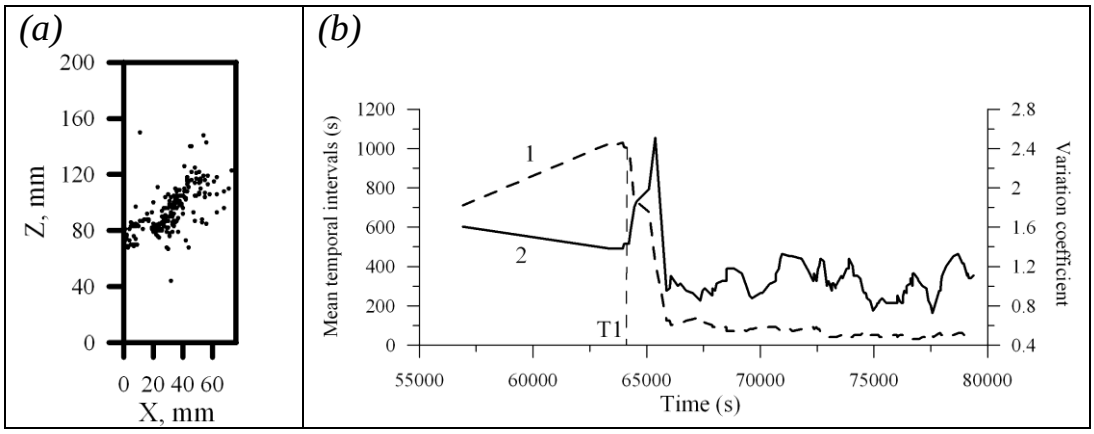

Fig.4. Defect accumulation in the water-saturated sample during deformation period I: (a) spatial distribution of coordinates of AE source hypocentres (b) variations in mean time interval (curve 1) and variation coefficient of time intervals (curve 2).

During loading period II, the picture is radically different (see Fig.5). Defect formation occurs in a disperse fashion throughout the entire sample volume (Fig.5a). Short mean time intervals are the consequence of the AE activity burst caused by the deformation increase. Then the time intervals grow. No simultaneous decrease in Δt and increase in $V_{\Delta t}$ pointing to formation of the fracture nucleation site are observed (Fig.5b). A further increase in load during period III does not lead to defect localization as well (Fig.6b).

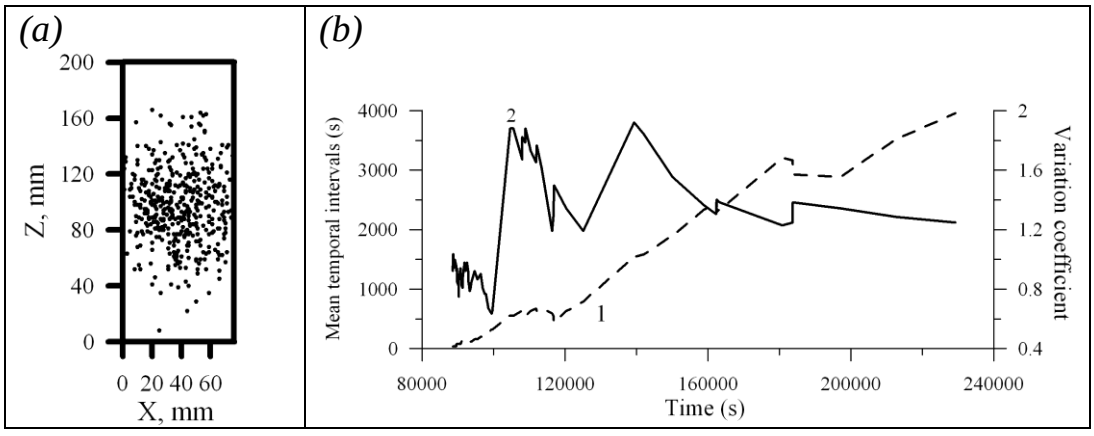

Fig.5. Defect accumulation in the water-saturated sample during deformation period II: (a) spatial distribution of coordinates of AE source hypocentres (b) variations in mean time intervals (curve 1) and variation coefficient of time intervals (curve 2).

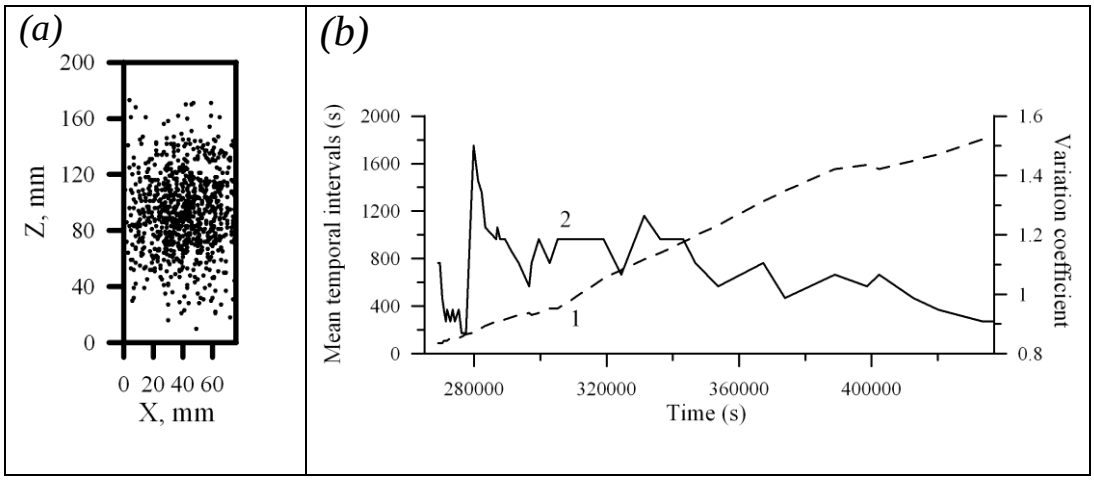

Fig.6. Defect accumulation in the water-saturated sample during deformation period III: (a) spatial distribution of coordinates of AE source hypocentres (b) variation in mean time intervals (curve 1) and variation coefficient of time intervals (curve 2).

Thus, it has been found that the defect accumulation proceeds in water-saturated samples in a fashion different from that in dry samples. In addition, it has been found that the deformation prior to sample breakdown for water-saturated sample is larger than that of the dry sample (Fig.7). This suggests that water has a plasticizing effect.

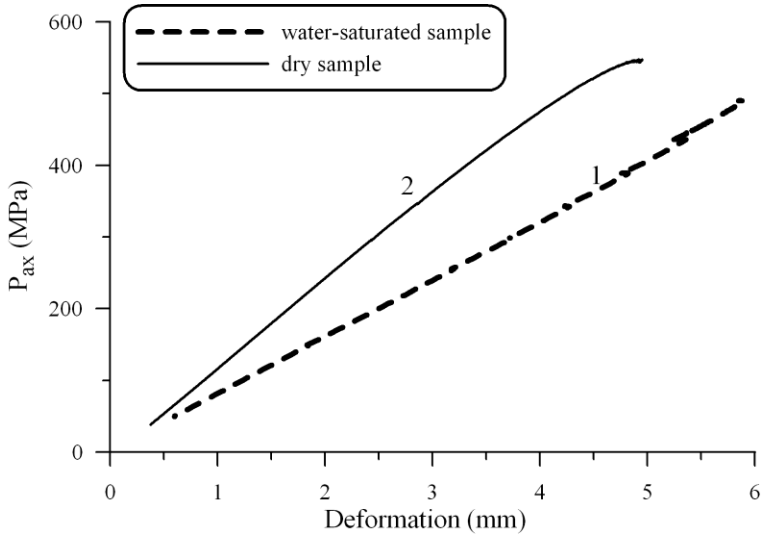

Fig.7. Axial load versus deformation: curve 1 - water-saturated sample, curve 2 - dry sample.

One of possible explanations of the plasticizing effect is as follows. Water molecules actively participate in hydrolytic scission of interactomic bonds [9]

$$Si\text{-}O\text{-}Si + H_2O \rightarrow Si\text{-}OH + HO\text{-}Si$$

The hydrolysis reaction proceeds under the action of external load even at room temperature. The hydrolytic mechanism leads to lowering of the activation energy for an elementary fracture act, which results in a lower strength of a material.

3. Conclusions

The mechanism of crack accumulation in water-saturated granite samples and its difference from crack accumulation in dry granite samples was studied. Defect generation was monitored by using the acoustic emission technique. It has been found that defect formation in the water-saturated samples occur uniformly throughout the sample volume, while loading of the dry sample results in a localized generation of defects giving rise to a fault. The interpretation of the difference between the crack accumulation patterns in water-saturated and dry samples can be as follows. Since all the pores in the water-saturated samples are filled with water, the strength at the pore-water interfaces decreases. One of possible explanations of this phenomenon is hydrolytic scission of interactomic bonds. Therefore, fracture of the water-saturated samples starts under lower stresses and takes place throughout the entire sample volume beginning from the pores, while in the dry sample the pores play an insignificant role in fault formation.

This work was supported by Russian Foundation for Basic Research (Grant N 07-05-00542).

References

1. G. A. Sobolev, Fundamentals of Earthquake Prediction, Nauka, Moscow, 1993.
2. V. V. Adushkin, S. B. Turuntaev, Man-Induced Processes in the Earth's Crust (Dangers and Catastrophes), INEK, Moscow, 2005.
3. S. A. Stanchits, D. A. Lockner, and A. V. Ponomarev, Anisotropic Changes in *P*-Wave Velocity and Attenuation during Deformation and Fluid Infiltration of Granite, Bulletin of the Seismological Society of America, 93 (4) (2003) 1803–1822
4. N. G. Tomilin, E. E. Damaskinskaya, P. I. Pavlov, Fracture of rocks as a multistage process, Fizika Zemli 8 (2005) 69-78

5. V. I. Myachkin, B. V. Kostrov, G. A. Sobolev, O.G. Shamina, Laboratory and theoretical investigations of the process of earthquake preparation, Izv. AN SSSR, Fizika Zemli 10 (1974) 2526-2530
6. V. S. Kuksenko, A. I. Lyashkov, K. M. Mirzoev et al. Relation between sizes of the cracks formed under load and duration of elastic energy release, Dokl. AN SSSR 264 (4) (1982) 846-848
7. N. G. Tomilin, E. E. Damaskinskaya, V. S. Kuksenko, Formation of a fracture focus during the deformation of heterogeneous materials (granite), Phys. Solid State 36 (10) (1994) 1649-1653
8. N. G. Tomilin, E. E. Damaskinskaya, P. I. Pavlov, Statistical kinetics of fracture of rocks and prediction of seismic events, Fiz. Tverd. Tela 47 (5) (2005) 955-959
9. V. A. Bershtein, V. V. Nikitin, V. A. Stepanov, L. M. Shamrey, Hydrolytical mechanism of fracture of glass under load, Fiz. Tverd. Tela 15 (11) (1973) 3260-3265